



Computational Science:
Introduction to Finite-Difference Time-Domain

Final Lecture

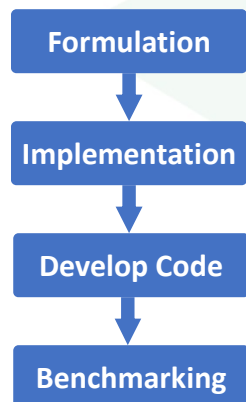
Lecture Outline

- Key points from course
- TE vs. TM
- Resonance hunting
- A good lesson -- Photonic crystals fabricated by multi-photon direct laser writing

Key Points From Course

Slide 3

Key Steps in the Art of Computational EM



Start with Maxwell's equations...

$$\begin{aligned} \nabla \times \vec{H} &= \vec{J} + \frac{\partial \vec{D}}{\partial t} & \nabla \cdot \vec{B} &= 0 & \vec{D} &= [\epsilon] \vec{E} \\ \nabla \times \vec{E} &= -\frac{\partial \vec{B}}{\partial t} & \nabla \cdot \vec{D} &= \rho_v & \vec{B} &= [\mu] \vec{H} \end{aligned}$$

Numerical approximation...

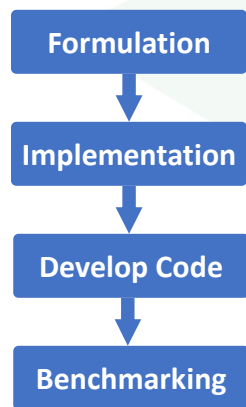
$$\begin{aligned} \frac{\partial H_x}{\partial t} &= -\frac{c_0}{\mu_{xx}} \left(\frac{\partial \tilde{E}_z}{\partial y} - \frac{\partial \tilde{E}_y}{\partial z} \right) \\ \downarrow \\ \frac{H_x|_{l+\frac{\Delta x}{2}}^{i,j,k} - H_x|_{l-\frac{\Delta x}{2}}^{i,j,k}}{\Delta t} &= -\frac{c_0}{\mu_{xx}|^{i,j,k}} \left(\frac{\tilde{E}_z|_l^{i,j+1,k} - \tilde{E}_z|_l^{i,j,k}}{\Delta y} - \frac{\tilde{E}_y|_l^{i,j,k+1} - \tilde{E}_y|_l^{i,j,k}}{\Delta z} \right) \end{aligned}$$

Derive update equations...

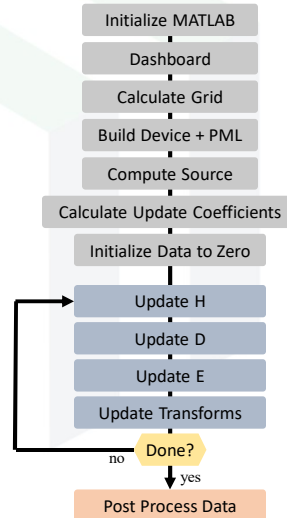
$$H_x|_{l+\frac{\Delta x}{2}}^{i,j,k} = H_x|_{l-\frac{\Delta x}{2}}^{i,j,k} - \frac{c_0 \Delta t}{\mu_{xx}|^{i,j,k}} \left(\frac{\tilde{E}_z|_l^{i,j+1,k} - \tilde{E}_z|_l^{i,j,k}}{\Delta y} - \frac{\tilde{E}_y|_l^{i,j,k+1} - \tilde{E}_y|_l^{i,j,k}}{\Delta z} \right)$$

Slide 4

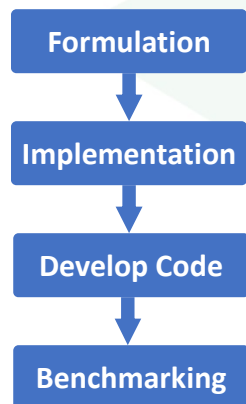
Key Steps in the Art of Computational EM



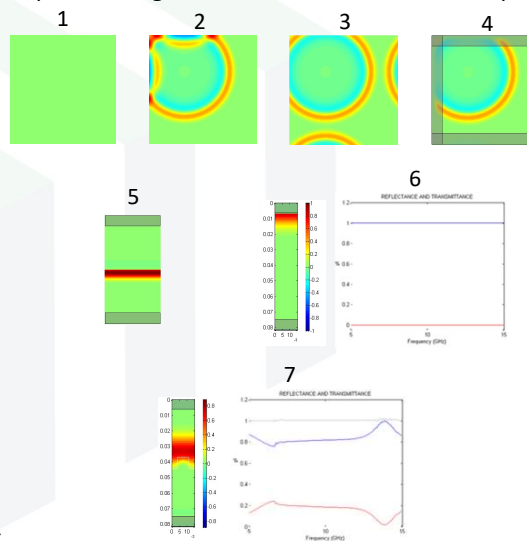
Outline algorithm, step-by-step...



Key Steps in the Art of Computational EM



Implement algorithm in small incremental steps...



Key Steps in the Art of Computational EM

```

graph TD
    A[Formulation] --> B[Implementation]
    B --> C[Develop Code]
    C --> D[Benchmarking]
    
```

Before you can trust your simulation results, you must duplicate known simulations.

$$\epsilon_2 = \sqrt{\epsilon_r \epsilon_{air}} = \sqrt{(12)(1)} = 3.46$$

$$n_2 = \sqrt{\epsilon_2} = \sqrt{3.46} = 1.86$$

$$\lambda_2 = \frac{c_0}{f_0} = \frac{299792458}{2.4 \times 10^9} = 12.49 \text{ cm}$$

$$d_1 = \frac{\lambda_2}{4n_2} = \frac{12.49}{4(1.86)} = 1.6779 \text{ cm}$$

$\Lambda = 1.5 \text{ cm}$
 $d = 0.75 \text{ cm}$
 $f = 50\%$
 $\epsilon_1 = 1.0$
 $\epsilon_2 = 9.0$
 $\epsilon_z = 1.0$
 $\epsilon_H = 9.0$

@ 10 GHz

100%
↓
EDTD

15.4% 51.1% 33.4% Total: 81.8%

100%
↓
RCWA

15.55% 50.46% 33.55% Total: 81.59%

RCWA provides "exact" solution.

Slide 7

Key Steps in the Art of Computational EM

The diagram shows a 3D perspective of the iterative process. It features a central vertical axis with three levels. Each level is represented by a grey rectangular block. The blocks are labeled with 'Practice' (in red), 'Benchmark' (in blue), and 'Small Steps' (in green). The labels are arranged in a repeating pattern: Practice, Benchmark, Small Steps, Practice, Benchmark, Small Steps, Practice, Benchmark, Small Steps. The blocks are slightly offset from each other, creating a sense of depth and progression.

Slide 8

Material Covered in This Course

- MATLAB
 - Basic commands and procedures
 - Graphics
 - Building devices on grids
- 1D FDTD
 - Formulation: Yee grid, finite-differences, update equations, update coefficients
 - Implementation: PAB, TF/SF, Fourier transforms, transmittance and reflectance, grid resolution
 - Generalizations: loss, dispersion
- 2D FDTD
 - Formulation: boundary conditions, PML, update equations, update coefficients
 - Implementation: PML, TF/SF, Fourier transforms, transmittance, reflectance
 - Generalizations: stretched coordinate PML, alternate grid schemes, waveguides, metals, periodic devices

Other Key Points

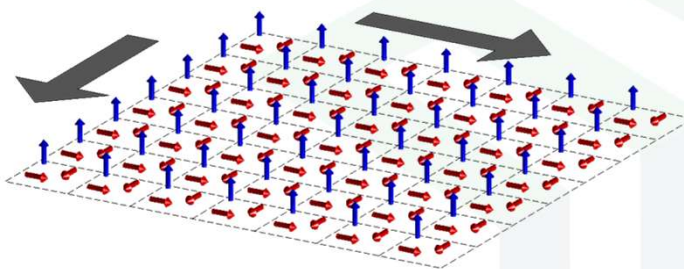
- Rhythm of deriving update coefficients
- Order of code development
- Art of representing devices on grids

TE vs. TM Modes in 2D Simulations

Slide 11

Framework #1 for the Definition of TE and TM

Orientation relative to direction of propagation

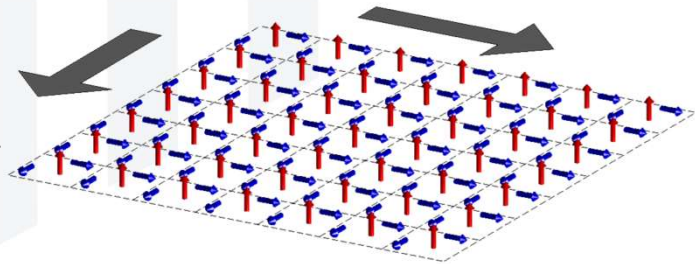


For the E_z mode, the electric field is always transverse to waves propagating in the x - y plane.

E_z Mode = TE Mode

For the H_z mode, the magnetic field is always transverse to waves propagating in the x - y plane.

H_z Mode = TM Mode



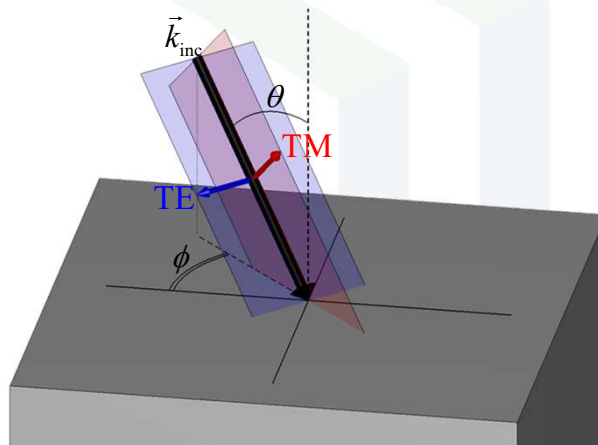
Slide 12

Framework #2 for the Definition of TE and TM

Orientation relative to the plane of incidence

TE – the electric field is polarized perpendicular to the plane of incidence.

TM – the electric field is polarized parallel to the plane of incidence.



In the limit as $\theta \rightarrow 90^\circ$, we have

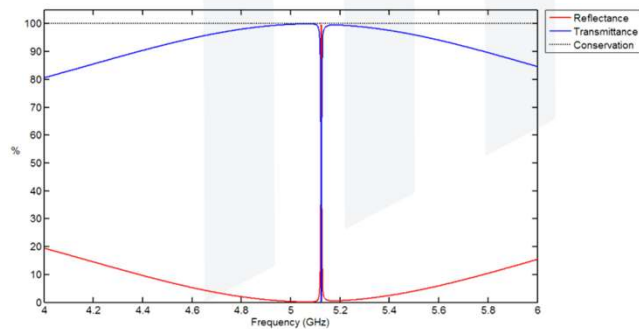
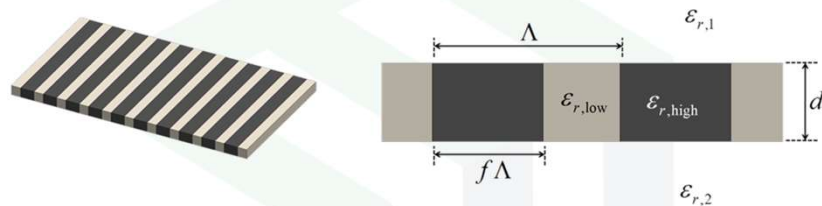
E_z Mode = TM Mode

H_z Mode = TE Mode

This is exactly the opposite of Framework #1 where propagation is restricted to be in the x - y plane.

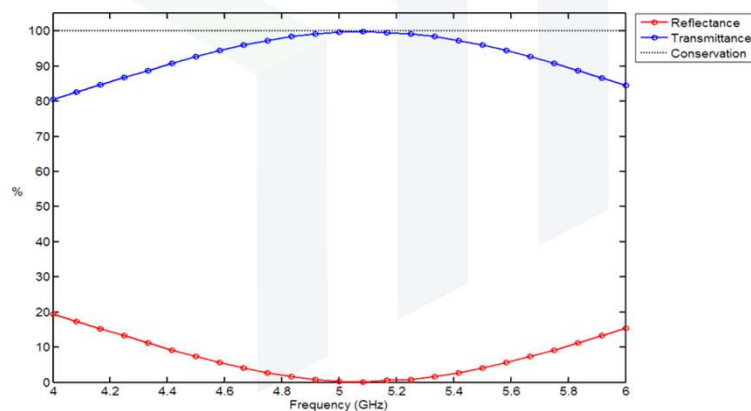
Resonance Hunting

Device for This Example



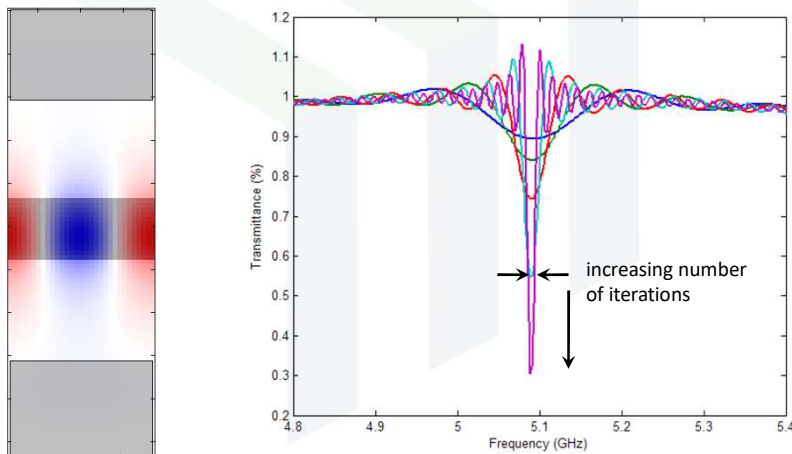
Results from a Frequency-Domain Method

Frequency-domain methods compute the field at one precise frequency from which transmittance and reflectance is calculated. If frequency points selected for the sweep are two widely spaced, narrow resonances are easily missed. Small frequency steps are very time consuming because many simulations have to be performed.



Results from a Time-Domain Method

Time-domain methods typically excite devices with all frequencies over a broad range. If a resonance exists, a time-domain method will detect it in a single simulation. It may take many iterations to resolve how narrow the resonance is, but the method will detect it almost immediately.



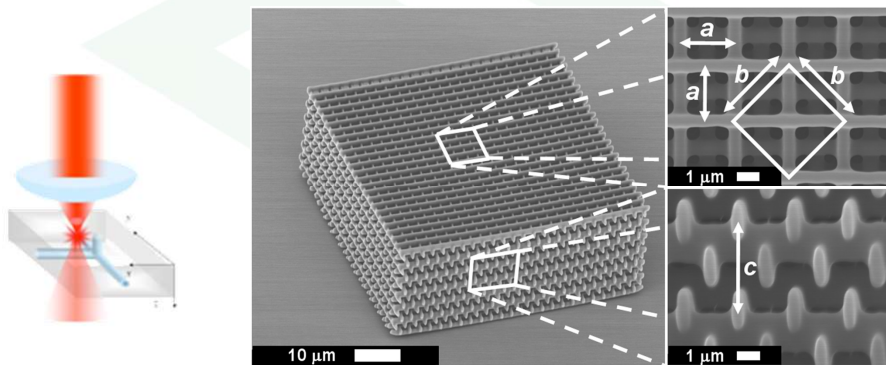
Conclusions

- Time-domain methods are excellent for identifying the existence of resonances.
- Time-domain methods are poor for resolving the shape of narrow resonances.
- Frequency-domain scattering methods are not reliable for finding narrow resonances. Visualizing the fields during a sweep can help this.
- Frequency-domain methods are excellent for resolving the shape of resonances.

Photonic Crystals Fabricated by Multi-Photon Lithography

Slide 19

Multi-Photon Lithography



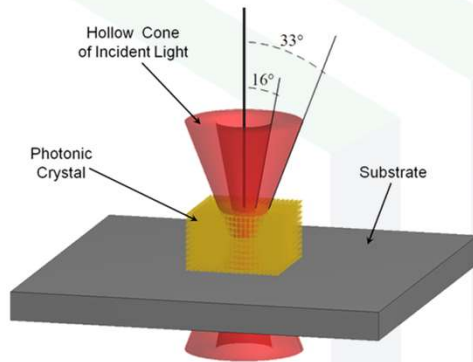
This is a scanning electron microscope image of a photonic crystal designed to operate in the infrared.



Slide 20

Fourier Transform Infrared Spectrometer

The Cassegrain optics illuminates samples with a "hollow" Gaussian beam.



Reflected infrared power at near normal reflection angle is collected and measured.



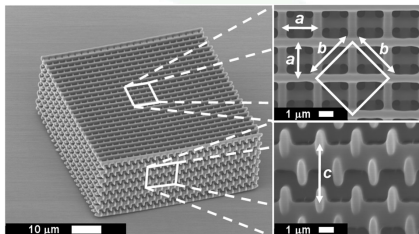
R. C. Rumpf, A. Tal, S. M. Kuebler, "Rigorous Electromagnetic Analysis of Volumetrically Complex Media Using the Slice Absorption Method," *J. Opt. Soc. Am. A* 24(10), 3123–3134 (2007).

EMPossible

Slide 21

Predicting Accurate Geometry

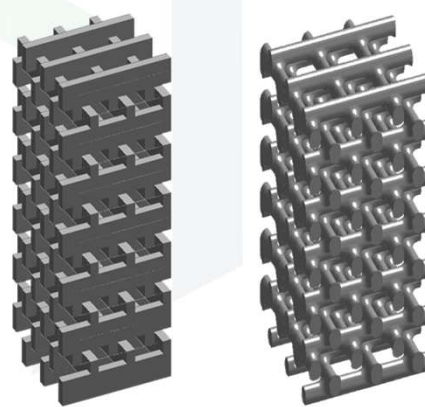
To predict the geometry of the photonic crystal more accurately, the DLW process was simulated in MATLAB.



R. C. Rumpf, A. Tal, S. M. Kuebler, "Rigorous Electromagnetic Analysis of Volumetrically Complex Media Using the Slice Absorption Method," *J. Opt. Soc. Am. A* 24(10), 3123–3134 (2007).



EMPossible

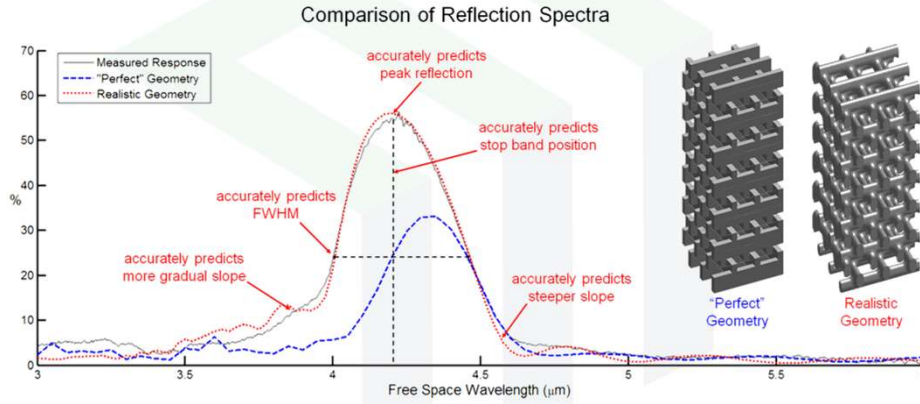


Idealized Geometry

Realistic Geometry

Slide 22

Importance of Realistic Geometry

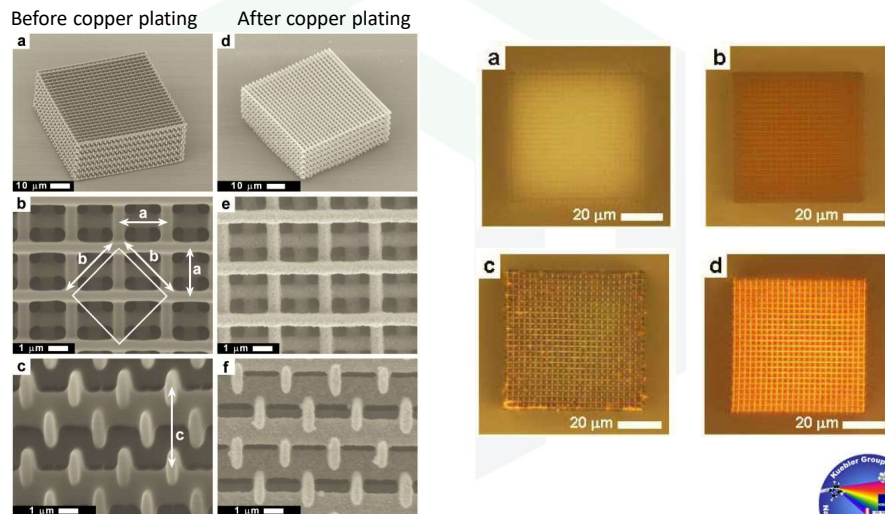


R. C. Rumpf, A. Tal, S. M. Kuebler, "Rigorous Electromagnetic Analysis of Volumetrically Complex Media Using the Slice Absorption Method," J. Opt. Soc. Am. A 24(10), 3123–3134 (2007).



Slide 23

Metallo-Dielectric Photonic Crystals



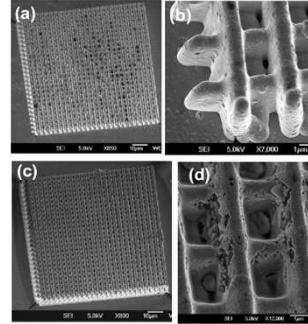
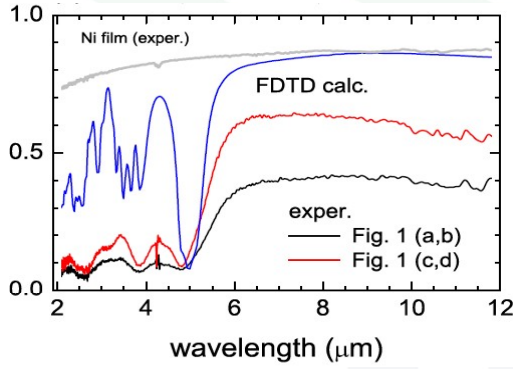
A. Tal, Y. Chen, H. Williams, R. C. Rumpf, S. Kuebler, "Fabrication and characterization of three-dimensional copper metallodielectric photonic crystals," Opt. Express 15(26), 18283-18293 (2007)



Slide 24

“State-of-the-Art” Simulation of Reflectance

Results obtained by Lumerical and Misawa’s research group.



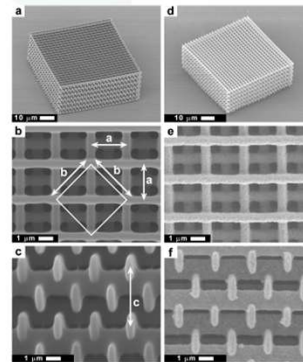
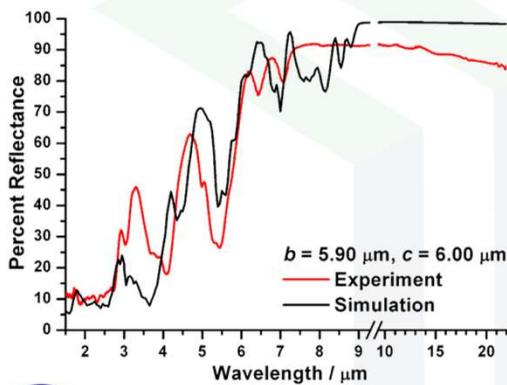
V. Mizeikis, S. Juodkazis, R. Tarozaitė, J. Juodkazyte, K. Juodkazis, H. Misawa, "Fabrication and properties of metallo-dielectric photonic crystal structures for infrared spectral region," Opt. Express 15, 8454-8464 (2007)



Slide 25

A Better Simulation of Reflectance

Results obtained by UCF/Rumpf team...



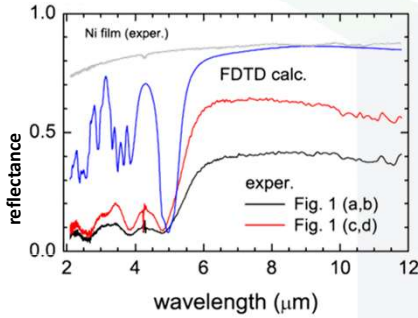
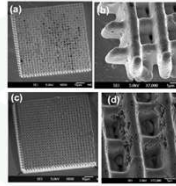
A. Tal, Y. -S. Chen, H. E. Williams, R. C. Rumpf, and S. M. Kuebler, "Fabrication and characterization of three-dimensional copper metallodielectric photonic crystals," Opt. Express 15, 18283-18293 (2007)



Slide 26

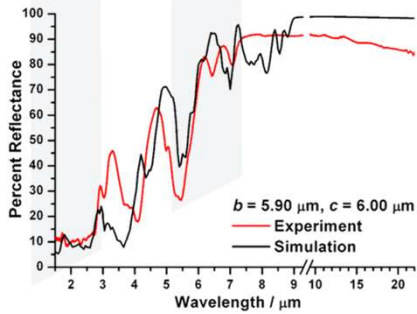
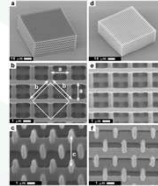
Side-by-Side Comparison

Results obtained with Lumerical's FDTD software



V. Mizeikis, S. Juodkazis, R. Tarozaitė, J. Juodkazyte, K. Juodkazis, H. Misawa, "Fabrication and properties of metallo-dielectric photonic crystal structures for infrared spectral region," Opt. Express 15, 8454-8464 (2007)

Results obtained by UCF/Rumpf

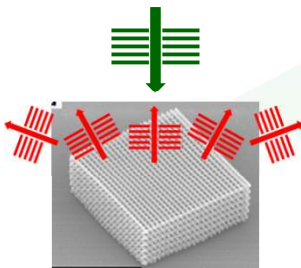


A. Tal, Y. -S. Chen, H. E. Williams, R. C. Rumpf, and S. M. Kuebler, "Fabrication and characterization of three-dimensional copper metallodielectric photonic crystals," Opt. Express 15, 18283-18293 (2007)



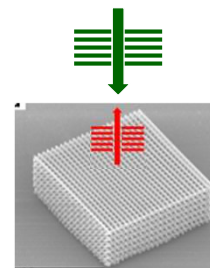
Slide 27

What May Have Been Their Mistake?



Below 10 μm (or so), this photonic crystal is a diffracting structure.

The optical configuration inside the FTIR cuts off the higher order modes. Essentially, it is only the zero-order diffracted mode that gets detected.



Slide 28